Research paper

Hydraulic architecture, height-related changes in photosynthesis, and seasonal positive pressure declines in bamboo: Implications for top dieback

Wen Guo[1], Jing-Qiu Feng[2], Jiao-Lin Zhang[3], Ze-Xin Fan[3], Pei-Li Fu[3], Hervé Cochard[4], Yong-Jiang Zhang[5, 6 *], Shi-Jian Yang[1, *]

[1]State Key Laboratory for Vegetation Structure, Function and Construction (VegLab), Ministry of Education Key Laboratory for Transboundary Ecosecurity of Southwest China, and Yunnan Key Laboratory of Plant Reproductive Adaptation and Evolutionary Ecology, Institute of Biodiversity, School of Ecology and Environmental Science, Yunnan University, Kunming, Yunnan 650500, China;

[2]College of Grassland Resources, Southwest Minzu University, Chengdu, Sichuan 610225, China;

[3]CAS Key Laboratory of Tropical Forest Ecology, Xishuangbanna Tropical Botanical Garden, Chinese Academy of Sciences, Mengla, Yunnan 666303, China;

[4]Université Clermont Auvergne, INRAE, PIAF, Clermont-Ferrand 63000, France;

[5]School of Biology and Ecology, University of Maine, Orono, ME 04469, USA;

[6]Climate Change Institute, University of Maine, Orono, ME 04469, USA.

* For correspondence: shijian.yang@ynu.edu.cn; yongjiang.zhang@maine.edu

Abstract

Background and Aims

Bamboos, arborescent monocotyledons without secondary growth, often show top dieback during the dry season. The potential mechanism underlying bamboo top dieback and its association with culm hydraulic architecture and positive pressure dynamics remain unclear. We investigated how the axial scaling of anatomical traits influenced physiological performances of the culm top under drought conditions, as well as how seasonal changes in positive pressure were related to top dieback and culm height.

Methods

Variations in culm anatomical and physiological characteristics (hydraulic traits, leaf photosynthetic gas exchange, and water potentials) along the longitudinal axis of a bamboo (*Dendrocalamus membranaceus*) were investigated and seasonal changes in positive pressure were monitored to reveal potential factors associated with top dieback.

Key Results

The hydraulically-weighted mean vessel diameters (D_h) exhibited a widening pattern from the culm apex with a scaling exponent in the range reported for trees. However, D_h did not increase continuously and instead declined noticeably near the culm base. Theoretical hydraulic conductivity decreased to a low level near the culm top, where most of the resistance was located. The lower water potentials, maximum quantum yield of photosystem II, stomatal conductance, and photosynthetic rate indicated that culm top was subjected to severer water stress than the base part. Height supported by the

maximum positive pressure declined from the wet season to the dry season, which was close to the measured culm height after top dieback.

Conclusions

This study implies the potential impact of vessel widening pattern on water supply along the culm height, and the association of seasonal changes in positive pressure with culm height, which offers novel insights into understanding bamboo top dieback.

Keywords:

culm height, hydraulic traits, leaf physiological traits, positive pressure, seasonal drought, top dieback, vessel widening

INTRODUCTION

Vascular plants can effectively transport water through xylem to the plant tops under normal conditions, keeping the canopy hydrated. This is achieved by optimizing the hydraulic architecture, which follows a pervasive pattern of tip-to-base xylem conduit widening (West *et al.*, 1999; Anfodillo *et al.*, 2006; Olson *et al.*, 2014). Conduits widen at a 'just right' rate during growth (known as the hydraulic optimality models), which may balance the increases in hydraulic resistance with conductive path length and vulnerability to embolism with conduit diameter if the conduits widen too slowly or rapidly (Anfodillo *et al.*, 2013; Olson and Rosell, 2013; Petit and Crivellaro, 2014; Olson *et al.*, 2021). The relationship between mean conduit diameter (D) and distance from the stem tip (L) follows a power function $D \propto L^b$, where b approaches 0.2 (Anfodillo *et al.*, 2006; Petit *et al.*, 2009; Lintunen and Kalliokoski, 2010; Bettiati *et al.*, 2012; Lechthaler *et al.*, 2019). Therefore, the conduits are narrowest at the stem tip and

widen very quickly near the tip, then widen slowly and continuously toward the stem base (Kiorapostolou *et al.*, 2018; Olson *et al.*, 2021). However, in some cases, the hydraulic benefits of conduit widening and photosynthetic return are not enough to offset the high carbon costs associated with building conduits with large diameters and thick walls, leading to no change or even a reduction in conduit size at a certain L (James *et al.*, 2003; Fan *et al.*, 2009; Petit *et al.*, 2010; Pfautsch *et al.*, 2018; Dória *et al.*, 2019; Aritsara and Cao, 2020). Narrowed conduits at the stem tip and increased path length can potentially limit efficient water supply to tissues at the top, which experience the lowest water potential within the individual and the highest risk of embolism (blockage of xylem conduits by air bubbles). Yet, how this hydraulic architectural design is related to top dieback under drought awaits further investigation, especially for arborescent monocots such as bamboos lacking secondary growth but showing substantial positive pressure.

When experiencing limited water supply, leaf abscission and twig necrosis often begin to appear at the tip in many plant species, that is, the phenomenon of top dieback (Mueller-Dombois, 1988; Davis *et al.*, 2002; Hentschel *et al.*, 2014; Pellizzari *et al.*, 2016; Savi *et al.*, 2019; Camarero, 2021). During the past decades, a large number of plant top dieback events have been reported worldwide and raised concerns about the consequent decrease in plant height and forest productivity with the increased incidence of drought (Nardini *et al.*, 2013; Hentschel *et al.*, 2014; Rosner *et al.*, 2016; Nolan *et al.*, 2021). Although a few studies suggest that the upper part of a plant seems to be more vulnerable to embolism than the base (Fang *et al.*, 2021), the underlying morphological and physiological mechanisms leading to plant top dieback ask for more studies. Bamboos are particularly prone to top dieback during the dry season (Kongjarat *et al.*,

2024). Given that drought is becoming longer, more frequent and more severe under global climate change (Dai, 2013; Ault, 2020), revealing the mechanisms underlying top dieback can aid in predicting bamboo response to increasing drought.

Top dieback could be associated with the narrowest conduits at the stem tip with relatively low hydraulic conductance (Fang *et al.*, 2021), which may result in insufficient water supply to leaf tissues under drought conditions. Branches near the stem top often experience the severest water stress during drought due to small conduit size, increased path length, and the accumulation of hydraulic resistance with plant height (Tyree and Zimmermann, 2002; Petit *et al.*, 2010; Pfautsch, 2016). Additionally, they are exposed to microenvironments with higher atmospheric water demand than the basal branches, resulting low water potentials that may cause xylem embolism (Davis *et al*., 2002; Xu *et al*., 2023). These factors together may bring hydraulic dysfunction and subsequent stomatal closure, photosynthetic inhibition, tissue desiccation, and branch shedding during water deficits. According to the hydraulic vulnerability segmentation hypothesis, the top dieback could be an adaptive phenomenon because it would allow trees to protect carbon costly proximal organs in drought periods by shedding the distal parts of xylem pathways to reduce path length and transpirational demand on conduit systems (Rood *et al.*, 2000; Pivovaroff *et al*., 2014; Anfodillo and Olson, 2021). The influence of the tip-to-base conduit widening pattern on plant physiological perforamnce and drought resistance needs further investigation.

To deal with occasional embolism events and maintain the maximum heights, plants have evolved diverse strategies. Bamboos with vascular bundles embedded in parenchyma tissue may use hydraulic capacitance to avoid xylem embolism. When embolism does happen, gymnosperm and dicotyledonous, can form new conduits

through the vascular cambium to replace impaired ones (Brodribb *et al.*, 2010; Trugman *et al.*, 2018). Whereas, in the absence of vascular cambium, positive pressure is the main mechanism that can actively refill embolized conduits (Cochard *et al.*, 1994; Saha *et al.*, 2009; Yang *et al.*, 2012; Schenk *et al.*, 2021). Monocots, especially their arborescent members (*e.g*. bamboos), usually adopt this strategy to ensure the hydraulic functions of conduits from the stem (culm) tip to base (Cao *et al.*, 2012; Yang *et al.*, 2015). Therefore, the value of positive pressure has a significant positive relationship with the maximum plant height in arborescent monocots (Cao *et al.*, 2012). Because positive pressure can be affected by soil water conditions (Stiller *et al.*, 2003; Singh, 2016; Gleason *et al.*, 2017; Drobnitch *et al.*, 2021; Fu *et al.*, 2022), seasonal changes in rainfall and soil water availability may influence the ability of arborescent monocots to supply water to the tops and keep their maximum heights. Declines in positive pressure could severely impede the refilling of potential xylem embolism at the top. As the arborescent monocots are important components of forests in tropical and temperate regions, there is a need to investigate how their maximum heights will respond to changes in positive pressure under changing climates.

In this study, a bamboo species *Dendrocalamus membranaceus* Munro, which often exhibited top dieback during the dry seasons (Figure S1), was chosen as a typical arborescent monocot to study its hydraulic architecture, examine how xylem anatomical and hydraulic traits change along the culm longitudinal axis, and test the potential association of culm hydraulic architecture and seasonal changes in positive pressure with top dieback and determining maximum bamboo culm height. Specifically, we hypothesized that: (1) conduit diameter (D_h) would increase from the culm tip to base following the hydraulic optimality models established for eudicots, but D_h would not

change or even decrease at the base; (2) due to the conduit widening pattern from the apex and increased path length, the lower water potentials of culm top would cause a more stressful water status relative to culm base, especially under drought conditions; and (3) with the decreasing soil moisture, positive pressure would decline during dry seasons, and the culm height after dry season top-dieback would equal to the height calculated by the dry season positive pressure.

MATERIALS AND METHODS

Study site and plant material

The present study was undertaken in a large bamboo collection at the Xishuangbanna Tropical Botanical Garden (XTBG, 21°56′N, 101°150′E; 570 m altitude) in Yunnan Province, SW China. In this region, there is a distinct dry season from November to April and a wet season from May to October. During the dry season, the climate is characterized by high temperature and vapor pressure deficit (VPD), with substantially reduced precipitation and soil volumetric water content (Figure S2) which measured by Time Domain Reflectometry (TDR-350 Soil Moisture Meter, Spectrum, Aurora, IL, USA).

Our target arborescent species, *Dendrocalamus membranaceus* Munro, a giant bamboo is typically found in tropical areas, particularly in Myanmar, Laos, Thailand, Vietnam and southern China. This kind of large clumping bamboo species has formed large natural bamboo forests in Southern China. For this study, all sampled culms were of similar age (3-year-old) to minimize age-driven variability. Ten individuals (culms) located in the bamboo common garden at XTBG were randomly selected, among which three culms were harvested for anatomical traits measurements, and the remaining four

and three culms were used for physiological traits and positive pressure in situ measurements, respectively.

Anatomical traits of bamboo culm

The actual height of three culms before and after dieback (Measured-H_{wet} and Measured-H_{dry}) were measured by a measuring tape in the wet and dry seasons. After the culm height reduction in the dry season, all branches and leaves were removed from the culm, and the sampled culms were sawn in the middle of each internode. For each culm, the cross-sectional discs of about 2 cm thickness were sawed manually in the middle of each internode from the tip to the base along the axial culm. For each sawed culm disk, the actual distance and relative distance from the culm tip (L; cm and %) along the axial culm were carefully recorded, transformed and normalized as a percentage form (%). Freshly excised culm segments were numbered, remarked, and wrapped in three big black plastic bags. Then, they were immediately transported to the laboratory for further anatomical measurements.

Culm diameter and culm wall thickness along the axial culm were determined by a measuring tape and an electronic digital caliper (Mitutoyo 500-196-30, Tokyo, Japan). In addition, the culm wall cross-sectional area and its ratio to the culm area of each culm segment were measured and calculated. The cross-sectional discs of each culm segment were prepared with different types of fine sandpaper to be flat, smooth, and clear enough until they were suitable for anatomical observations under a stereo microscope (Leica M50, Wetzlar, Germany). The surface contrast of the cross sections was enhanced with very fine, white chalk powder after the surfaces of the cross sections were stained with 1% safranin solution for 5 minutes. Then, the culm cross-sectional

discs were observed under the aforementioned stereo microscope. Digital images were captured by a connected digital camera (Leica IC80 HD, Wetzlar, Germany) at ×10, ×16, ×25, and ×40 magnifications, respectively. In order to get the anatomical traits of the entire cross-section, overlapping images covering the whole cross-sectional area were stitched with PTGUIPRO software (New House Internet Service B.V., Rotterdam, The Netherlands), then scaled and analyzed with Image J (http://rsb.info.nih.gov/ij/). Culm anatomical traits, such as the cross-sectional area of each vessel and parenchyma, the diameter of all vessels, and the number of vessels with different lumen diameters, were measured and estimated in several views with a known area. Lastly, the area ratio of the vessel and parenchyma of the total area of each cross-section, and the vessel density in the sampled cross-sectional discs of each culm were calculated, respectively.

Hydraulic and wood properties of bamboo culm

All vessels of bamboo culm were considered to be circular and the hydraulically-weighted mean vessel diameter (D_h) was assessed for each image as

$$D_h = (\sum D^4/N)^{1/4}$$

where D is the mean vessel diameter and N is the number of vessels in the image (Tyree and Zimmermann, 2002; Choat *et al.*, 2007).

The theoretical hydraulic conductivity (theoretical K_h) of the vessels in the culm wall was calculated according to the following Hagen-Poiseuille equation:

$$\text{theoretical } K_h = (D_h^4 \pi \rho)/128\eta \times \text{VD}$$

Where ρ is the density of water at 20°C (998.2 kg m^{-3}), η is the viscosity of water at 20°C (1.002×10^{-9} MPa s), D_h is the hydraulically-weighted mean vessel diameter, and VD is the vessel density (Choat *et al.*, 2007; Fichot *et al.*, 2010). The theoretical

sapwood-specific hydraulic conductivity (theoretical K_s) was estimated as theoretical K_h scaled per unit sapwood area (the culm wall cross-sectional area, here).

The resistance (r) of a single vessel within each bamboo internode is given by the equation:

$$r = \frac{128 \times \eta \times l}{\pi \times d^4}$$

where η = water viscosity (1.002×10^{-9} MPa s) at 20 °C, l = 0.1 cm long employed in each segment, and d = vessel diameter (Tyree and Zimmermann 2002; Petit *et al*., 2008; Williams *et al*., 2019). The hydraulic resistance (R) of all vessels within any culm segment (k) is the inverse sum of hydraulic conductivity (1/r) of each single vessel. With considering the resistance of successive vessels connected in series and assuming no vessel furcation, the cumulated total theoretical hydraulic resistance (R_{tot}) from the base (Level 0) to top (Level N) through successive culm segments is calculated as $R_{tot} = \sum_{k=0}^{N} R_k$ (Becker *et al*., 2000; Petit *et al*., 2010).

For culm wood density (WD) along the culm axial height, 2-cm-thick culm segment samples were collected from the middle part of each internode after labeling the relative distance from the culm tip. Culm segment samples were immersed in distilled water to obtain the fresh volume using Archimedes' immersion method. Dry weight was determined after all the culm segment samples were dried to a constant weight at 80°C for 72 h. Culm WD was calculated as the ratio of dry weight to the fresh volume of the culm segment samples.

Leaf physiological traits

During the dry season, four individuals showed top dieback were selected for physiological traits measurements. Each individual was divided into seven or eight

height intervals from top to bottom along the culm. By using a manual lift truck (Figure S1), we can access each height to measure leaf photosynthetic gas exchange *in situ* and collect samples for leaf water potential and trait measurments. At each height, we measured five fully expanded leaves.

A portable infrared gas analyzer (LI-6800, LI-COR, Lincoln, NE, USA) with a blue-red light source was used to measure leaf gas exchange. All measurements were performed in the morning between 09:00 and 11:30 h. Irradiance, CO_2 concentration, temperature, and relative humidity inside the leaf chamber of the gas-exchange system were maintained at 1200 μmol m^{-2} s^{-1}, 400 ppm, 25 ± 1 °C, and 70%–80%, respectively. We recorded the maximum photosynthetic rate (A_{max}), stomatal conductance (g_s), and transpiration rate (E) for each leaf after the intercellular CO_2 concentration was stabilized. Instantaneous water-use efficiency (WUE_i) was calculated as the ratio of maximum photosynthetic rate and transpiration rate (A_{max}/E).

Chlorophyll fluorescence was measured between 06:00 and 06:30 h on leaves that had been dark-adapted overnight on the following day of leaf gas exchange measurements. A portable fluorometer FluorPen (FP 110, Photon Systems Instruments, Drásov, Czech Republic) was used to measure the maximum quantum yield of photosystem II (PSII) ($F_v/F_m = (F_m - F_o)/F_m$). At least five replicates for each height interval were made.

For leaf water potential, three small shoots at each height were cut and placed in sealed plastic bags until water potential measurements were taken in a lab nearby. Shoots were approximately 20 cm in length with 3–5 leaves and intact septa between nodes. The leaf water potential at predawn (Ψ_{pre}) and midday (Ψ_{mid}) was measured using a pressure chamber (PMS1505D, PMS Instrument, Albany, OR, USA). The predawn

water potential (Ψ_{pre}) was determined in the early morning (06:00–07:00 h) before sunrise and transpiration, and midday water potential (Ψ_{mid}) was measured at noon (13:00–14:00 h) on sunny days.

Following water potential measurements, leaves on the small shoots were collected to determine leaf size (single leaf area, A_L) and leaf dry mass per unit area (LMA). The leaves were scanned using a scanner (CanoScan LiDE300, Canon, Japan) and leaf areas were estimated by ImageJ V1.45 (Schneider *et al.*, 2012). Leaves were dried at 65 °C for 48 h and weighed to calculate LMA (leaf dry mass/leaf area).

Seasonal changes of positive pressure

In February and August (representing the dry and wet seasons, respectively), the dynamics of positive pressure from three individuals were simultaneously measured using digital pressure transducers (PX26-100DV, Omega Engineering, Stamford, CT, USA) on consecutive sunny days (Figure S4). A small branch at the bottom (approximately 1 m above the ground) of the mature culm was selected and cut by a scissor at dusk. The cross section of the branch stump was re-cut with a fresh razor blade. Then, a single pressure transducer connected to a silicone tube filled with distilled water was fitted to the branch stump using zip-ties. The xylem pressure was recorded at a 10 min interval automatically with a data logger (CR1000, Campbell Scientific, Logan, UT, USA). Positive pressure was the xylem pressure recorded at the cut end of the small branch stump, plus the hydrostatic pressure generated by the water column from the ground to the small branch stump. The maximum positive pressures monitored in the dry and wet seasons were used to calculate the height limitation of bamboo culms (Calculated-H_{dry} and Calculated-H_{wet}) based on the assumption that bamboos need to

use positive pressure to push water to the top of the culm and positive pressure determines bamboo height (Cao *et al*., 2012). Thus, the estimated maximum height equals to the height (h) of water column maintained by the maximum positive pressure. The height (h) can be derived from the liquid pressure formula $P = \rho gh$, where P is the maximum positive pressure, ρ is the water density, and g is the gravitational acceleration.

Statistical analysis

For each individual culm, the different relative distance from the culm tip (L) to each culm segment was carefully calculated and normalized by their actual maximum height. Culm anatomical and hydraulic parameters at different actual (absolute) or relative distances from the culm tip (L; cm or %) were averaged for the four orientations of each culm segment. We used exponent or linear regression analysis to fit the relationships wherever possible. Regression coefficients, the 95% confidence intervals (CIs), and the 95% prediction intervals (PIs) were computed using SigmaPlot 10.0 (Systat Software, SPSS Inc., Chicago, IL, USA). We also conducted *t*-tests for the maximum positive pressure across the two seasons, between Measured-H_{dry} and Calculated-H_{dry}, and between Measured-H_{wet} and Calculated-H_{wet}, using SPSS 20.0 software (IBM, New York, USA), respectively. Then, Tukey's comparison tests were applied to assess the differences significance at $\alpha = 0.05$ level.

RESULTS

Axial variation of anatomical and hydraulic traits

The hydraulically-weighted mean vessel diameter (D_h) of the bamboo species showed a

basipetal widening pattern that generally followed a power-law scaling relationship with the distance from the culm tip (L). However, this widening trend was interrupted within the basal 20% of the culm length, where conduit diameters transitioned to a narrowing profile (Figure 1). The axial increasing pattern in D_h not only followed a linear log relationship along the culm (Figure 1, the inset), but was well-fitted by the power functions, which explained 94-96% of the total variance (Table 1). The three sampled culm individuals showed similar degrees of axial conduit widening, with the scaling exponent (b) that varied near 0.17 (Table 1).

The vessel area ratio showed a decreasing trend with the increase of relative distance from the culm tip (L), from 8.4% to 2.3% (Figure 2a). The vessel area ratio was also negatively correlated with the parenchyma area ratio in the culm wall transverse sections (Figure 2a, the inset). While vessel number increased linearly with relative L for each cross-section (Figure 2c), vessel density decreased from the culm tip to base, ranging from 12.7 to 2.3 no. mm^{-2} (Figure 2b). The maximum vessel diameters (D_{max}) increased from the culm tip to ca. 80% of relative L and then decreased, thus the widest D_{max} was not observed at the culm base (Figure 2d).

A pronounced curvilinear pattern of theoretical hydraulic conductivity (K_h) was detected along the axial culm, with the lowest value at the tip and the peak at ca. 80% of relative L (Figure 3a). However, theoretical sapwood-specific hydraulic conductivity (K_s) decreased from the culm tip to the base (Figure 3b). Accumulating from the basal culm upwards, total theoretical hydraulic resistance (R_{tot}) increased along the culm (Figure 3c), and the most pronounced change in resistance of each internode (R) occurred near the culm top (Figure 3c, inset). Similarly, wood density (WD) also increased upwards. from 0.67 to 0.91 g cm^{-3} (Figure 3d).

From tip to base, culm diameter increased 3.6-fold (17.5 to 62.7 mm; Figure S3a), while culm wall thickness showed a nonlinear 5.9-fold increase (3.1 to 18.3 mm; Figure S3b). Internode length exhibited a complex curvilinear pattern, initially increasing before reaching a plateau and subsequently decreasing (Figure S3c). The culm wall cross-sectional area increased dramatically by 38-fold (0.7 to 26.8 cm^2; Figure S3d), reflecting its hollow cylindrical structure analogous to tree sapwood.

Axial variation of leaf physiological traits during the dry season

A sharp decline in the maximum quantum yield of photosystem II (F_v/F_m) as the distance from the tip decreases was observed in the upper part of the culm (from 20% of relative distance to the tip, Figure 4a). Leaf dry mass per unit area (LMA) increased upwards within the culm from 50% of relative distance to the tip, while leaf size (A_L) decreased in the apical direction (Figure 4b). Both predawn (Ψ_{pre}) and midday leaf water potential (Ψ_{mid}) increased with the increasing distance from the culm tip (Figure 4c, d). Ψ_{mid} decreased from -3.67 MPa at 70% of relative distance to -4.89 MPa at the tip (Figure 4d).

The maximum photosynthetic rate (A_{max}) and stomatal conductance (g_s) were smallest in the upper part of the culm, increased substantially in the middle, and tended to decrease in the lower part (Figure 5a, b). Transpiration rate (E) exhibited an increasing trend from the culm tip to the base (Figure 5c), while instantaneous water-use efficiency (WUE_i) exhibited the opposite trend (Figure 5d).

Culm height and positive pressure in the dry and wet seasons

The maximum positive pressure reduced from 151.6±3.3 kPa in the wet season to 124.3±3.3 kPa in the dry season (the inset in Figure 6 and Figure S4). Seasonal drought-triggered shoot dieback was observed at the bamboo culm top (Figure S1), which caused terminal branches shedding and culm height reduction. Thus, the measured height of the culm apex in the dry season (Measured-H_{dry}) was lower than that (Measured-H_{wet}) in the wet season (Figure 6). The heights calculated based on maximum positive pressure in the wet (Calculated-H_{wet}) and dry seasons (Calculated-H_{dry}) were close to the measured culm heights in the wet and dry seasons respectively (Figure 6).

DISCUSSION

Our study demonstrates that the culm hydraulic architecture of the bamboo species is overall in line with the hydraulic optimality models, while it achieved this without secondary growth. Interestingly, the tip-to-base widening pattern of D_h is not continuous, and exhibits a declining trend close to the base, which warrants future investigation into its adaptive significance. The culm hydraulic architecture and leaf physiological traits of this bamboo species also suggests that culm top is susceptible to drought stress due to the tip-to-base widening hydraulic design and low water potentials at the top. Further, water stress of the top is exacerbated by declines in positive pressure during the dry season. Declines in positive pressure may impede the refilling of the water storage pool and possible xylem embolism in the dry season, potentially leading to enhanced water deficits and dieback at the top. However, further studies should combine visualization methods such as the micro-CT and optical methods (Kongjarat *et al.*, 2024) with xylem pressure measurements to estimate the critical thresholds of

embolism occurrence and potential refilling by xylem pressures at different culm height. Previous evidence from the decline and recovery of leaf hydraulic conductance in bamboo (Yang *et al*., 2012) may not be related to xylem embolism (Schenk *et al*., 2021). Our study thus provides a possible explanation for the commonly-found top dieback in bamboos in terms of culm hydraulic architecture and seasonal declines in positive pressure, asking for further physiological studies.

Hydraulic architecture and axial vessel widening in bamboo culm

Our findings that the hydraulically-weighted mean vessel diameter (D_h) increases with the distance from culm tip (L), are in line with the hydraulic optimality models. The conduit widening exponents (b) of three *D. membranaceus* individuals were approximately equal to 0.2 regardless of their heights, suggesting stability of the widening pattern among different individuals. Anatomical studies that investigated the conduit diameter scaling with plant height provided strong evidence for the stability of widening exponents across various clades, ontogenetic stages, and life forms including trees, shrubs, succulents, lianas, arborescent monocots, etc. (West *et al.*, 1999; Anfodillo *et al.*, 2006; Petit *et al.*, 2014; Pfautsch, 2016; Rosell *et al.*, 2017; Prendin *et al.*, 2018a; Olson *et al.*, 2021). In addition, plants under different environmental settings (*e.g.* temperature, precipitation, CO_2, nutrient availability) and vigor degrees also showed a similar relationship between D_h and L (Olson *et al.*, 2013; Prendin *et al.*, 2018b; Lechthaler *et al.*, 2019; Fajardo *et al.*, 2020; Kiorapostolou *et al.*, 2020; Rita *et al.*, 2024). Such widespread convergence on an exponent of about 0.2 indicates that vascular designs with conduits widening at this 'just right' exponent should be adaptative for plants (Anfodillo *et al.*, 2013; Olson *et al.*, 2014; Koçillari *et al.*, 2021). On the one

hand, conduit widening might buffer the accumulation of hydraulic resistance with plant height and allow leaves at different *L* to maintain a constant hydraulic conductance (Becker *et al.*, 2000; Petit *et al.*, 2008; Echeverría *et al.*, 2019; Yang *et al.*, 2021). On the other hand, this 'just right' widening pattern (b = 0.2) might avoid overbuilt large vessels at the base (b > 0.2), reducing the risk of drought/freezing-induced xylem embolism and conduit wall construction costs (Mencuccini *et al.*, 2007; Olson *et al.*, 2018).

Consistent with our hypothesis, D_h did not increase continuously, but rather, showed an obvious declining trend close to the culm base. Similar findings had also been reported in other plants such as a shrub, eucalypts and palms (Petit *et al.*, 2010; Pfautsch *et al.*, 2018; Dória *et al.*, 2019; Aritsara and Cao, 2020). While a continuous tip-to-base widening of conduits is widely accepted in the literature (Anfodillo *et al.*, 2006; Rosell *et al.*, 2017; Olson *et al.*, 2021), we can explain the growing evidence of a narrowing trend near the stem base with various factors. Including a sufficient number of sampling points (especially at the base) help to reveal the overall trend of conduit diameter along the whole plant height (Soriano *et al.*, 2020). Interestingly, bamboos, as monocots without secondary growth, pre-determine this vessel size distribution pattern at the early primary growth stage. It seems monocots are programmed to 'know' the final height and form the vessel size distribution pattern accordingly at the early development stage (Petit *et al.*, 2014; Yang *et al.*, 2021), with the detailed regulation mechanism and impacts on physiological performances relatively unknown. Physiological causes may be related to the constraints on hydraulic efficiency and the high carbon investment if conduits are still widening toward the base. First, wider conduits at the base would increase the volume of xylem water in the plant transportation

system, which has been suggested to reduce the efficiency of the water distribution network due to the large volume of water needed to fill the base water pool (Banavar *et al.*, 1999). Second, larger conduits at the stem base may provide negligible benefit to the hydraulic efficiency of the whole plant (Petit *et al.*, 2010; Prendin *et al.*, 2018a), since the majority of hydraulic resistance is concentrated near the top where the conduits are narrowest (Petit and Anfodillo, 2009; Lechthaler *et al.*, 2020). Additionally, such a small hydraulic benefit may not offset the carbon costs for constructing and maintaining larger conduits (Mencuccini *et al.*, 2007; Hölttä *et al.*, 2011). Therefore, basal conduit narrowing suggests a limitation to the hydraulic compensation mechanism by axial conduit widening (Williams *et al.*, 2019). The pronounced narrowing observed at the culm base, which coincides with rhizome connections, highlights a critical functional interface between belowground and aboveground hydraulic systems. This structural feature underscores the need for investigation into this junction of hydraulic continuity.

Axial scaling of physiological traits reflects water stress at the culm top during the dry season

The trends of physiological traits along the longitudinal axis of the bamboo culm showed a clear divergence between the top and the base, with the top experiencing strong water stress during the dry season. As conduit diameter contributed to a large portion of the hydraulic resistance (Becker *et al.*, 2003; Petit *et al.*, 2010; Williams *et al.*, 2019; Lechthaler *et al.*, 2020), the vast majority of total hydraulic resistance (R_{tot}) was located towards the culm top where xylem conduits tapered more sharply (Petit and Anfodillo, 2009; Lechthaler *et al.*, 2020). This, in combination with increased path length for water transport, constrained the theoretical hydraulic conductivity (K_h) to be

at a low level near the culm top (Pfautsch *et al*., 2018; Yang *et al*., 2021). Similarly, in *Populus* trees, the practical measurement of K_h also showed a sharp decrease in the apical branches (Fang *et al.*, 2021). We recognize that xylem vessel diameter alone does not solely determine water transport. Other xylem characteristics, such as vessel length, may also significantly influence hydraulic conductance (Comstock and Sperry, 2000; Jacobsen *et al*., 2012), although this aspect was not investigated in the present study.

When water supply from the soil was limited, maintaining apical branches hydrated with low K_h became increasingly difficult because increased xylem tensions may intensify the limitations on water flow, dropping water potentials (Ψ_{pre} and Ψ_{mid}) and further increase water stress of the culm top (Xu *et al.*, 2023). Lower maximum quantum yield of photosystem II (F_v/F_m) at the tip (0.65) also supported the idea that culm top was subjected to severer water stress than the base part. Meanwhile, upper leaves exhibited remarkable decreases in stomatal conductance (g_s), transpiration rate (E) and leaf photosynthesis (A_{max}) with sampling heights near the culm top. This could result in carbon imbalance (declined or limited carbon return on input in stem and leaf biomass), which is used to explain tree top and individual dieback (Zhang *et al.*, 2009). Although previous studies showed that leaf photosynthesis increased with heights within an individual or across different species (Ellsworth and Reich, 1993; Kenzo *et al*., 2015), reflecting acclimation to vertical trend of increasing light from bottom towards treetop, similar lower rates of photosynthesis for upper leaves were often observed in water-limited environments (*e.g*. tropical dry forest) (Zhang *et al.*, 2009; Kenzo *et al*., 2012; Jin *et al*., 2024). Since our physiological measurements were conducted only during the dry season (due to the acute onset of dieback symptoms), future studies comparing irrigated and drought-affected individuals (Xu *et al.*, 2023) or

incorporating seasonal monitoring (Kongjarat *et al.*, 2024) could help establish causal links between physiological decline and top dieback.

The bamboo *D. membranaceus* also exhibited trait adjustments to mitigate the effects of increased water stress at culm top like other tree species (Choat *et al.*, 2005; Domec *et al.*, 2008). At the leaf level, mature leaves became smaller and thicker, while dry mass per unit area (LMA) increased upwards (Koch *et al.*, 2004), which may resist collapse caused by a low water potential and contribute to high drought tolerance of upper leaves (Woodruff *et al.*, 2004; Williams *et al.*, 2017). By controlling stomatal conductance, the upper leaves could minimize transpiration consumption and improve leaf water use efficiency (WUE), and a high WUE was important to advantageous photosynthetic production under drought conditions. At the branch level, an increase in sapwood-specific conductivity (K_s) resulted from a lower rate of decline in K_h relative to the sapwood area, a pattern also observed in *Sequoia sempervirens* (Burgess *et al.*, 2006), indicating partial compensation for hydraulic limitation. In this context, dieback of top branches could prevent further water loss and protect more carbon-costly organs by shedding terminal organs according to the theory of hydraulic segmentation (Pivovaroff *et al.*, 2014), thus enhancing survival at the whole-tree level.

Anatomical traits of the culm base were associated with mechanical support and water storage. Compared with the culm top, the base part was composed of thicker culm walls and higher culm wall cross-sectional areas (Figure S3), which could provide strong physical support (Aritsara and Cao, 2020). The highest parenchyma area ratio was accompanied by decreases in vessel area ratio and wood density at the culm base, which reflected a large volume for storage of water and non-structural carbohydrates (Plavcová *et al.*, 2016). This large parenchyma area ratio could provide a reservoir to

buffer the daily water loss by leaf transpiration (Yang *et al.*, 2015; Williams *et al.*, 2021). Therefore, the culm base was the part less likely susceptible to water stress relative to the culm top.

Seasonal positive pressure changes influence the maximum culm height

The observed decline in positive pressure during the dry season in bamboo likely reflects a dynamic interplay between environmental stressors and regulation of pressure generation. The maximal positive pressure of *D. membranaceus* decreased (Figure 6 and Figure S4) as soil moisture declined and vapor pressure deficit (VPD) increased (Figure S2). This aligns with previous studies showing that episodic pressure patterns are strongly influenced by soil moisture (Singh, 2016; Gleason *et al.*, 2017; Drobnitch *et al.*, 2021; Fu *et al.*, 2022) and atmospheric demand (Michaud *et al.*, 2024), which underscores the sensitivity of pressure generation to ambient humidity. Traditional studies have postulated that xylem positive pressure originates from root, where changes in soil humidity alter aquaporin activities in roots, thereby regulating water influx and subsequent pressure generation (Singh, 2016; Schenk *et al.*, 2021). However, recent work by Michaud *et al.* (2024) challenges this assumption by demonstrating that stems and rhizomes of bamboos can generate positive pressure, a process that may involve mechanical swelling in tissues such as phloem, parenchyma, or fibres. In light of these findings, the observed pressure decline may also reflect differential stem water status and tissue rehydration capacity under varying water conditions.

During the dry season, the decreased maximum positive pressure could serve as an indicator of water scarcity, indicating insufficient soil moisture to sustain hydraulic recovery. Positive pressure can dissolve conduit embolisms and restore xylem function

(Knipfer *et al.*, 2015; Gleason *et al.*, 2017; Schenk *et al.*, 2021). This is an important physiological mechanism of hydraulic recovery in many plant groups, especially for monocots (*e.g.* bamboos) that have no secondary growth to replace embolized conduits (Cochard *et al.*, 1994; Stiller *et al.*, 2003; Saha *et al.*, 2009; Yang *et al.*, 2012). In arborescent monocots such as bamboos, positive pressure declines with culm height, reaching near-zero values at the apex due to the gravitational pressure (Cao *et al.*, 2012). This axial reduction in positive pressure along the culm limits hydraulic recovery in upper regions, as refilling embolized xylem conduits requires overcoming gravitational and hydraulic constraints. Here we assume that maintaining the xylem fluid pressure at zero MPa is sufficient to refill xylem embolism. Some previous studies have found that atmospheric pressure is indeed sufficient to refill leaf xylem embolism with enough time (Subczynski *et al.*, 1992; Hochberg *et al.*, 2016; Knipfer *et al.*, 2016; Yang *et al.*, 2024). However, when seasonal declines in positive pressure occur during drought periods, combined with multiple hydraulic constraints (*e.g.*, tapered conduit architecture, elevated atmospheric demand, and impaired tissue rehydration), pressure values at the apex may drop further, thereby exacerbating hydraulic dysfunction in apical regions. Thus, a clear relationship exists between bamboo's positive pressure and culm height across seasons (Figure 6). The high positive pressure of *D. membranaceus* in the wet season could pump water to a height (Calculated-H_{wet}) close to its maximum culm height (Measured-H_{wet}), which allowed culms to refill the xylem embolisms at the top. However, the height of the water column supported by the maximum positive pressure in the dry season (Calculated-H_{dry}) was lower than that in wet season, resulting in a lack of refilling of the bamboo terminal shoots above Calculated-H_{dry}. In line with our hypothesis, Calculated-H_{dry} was close to measured culm height in the dry season

(Measured-H_{dry}), which provided an implication on the role of decreased positive pressure in top dieback. Additionally, because nocturnal sap flow driven by positive pressure is important in recharging the water storage (Yang *et al.*, 2015), declined maximum positive pressure in the dry season may also impede the refilling of water storage at the top. While reduced positive pressure may partially account for top dieback, it likely operates within a complex framework of environmental and physiological stressors. Under climate change-driven extreme drought conditions, diminished positive pressure likely interacts with broader hydraulic impairments exacerbating top dieback and mortality that critically undermine bamboo forest productivity.

CONCLUSIONS

In summary, the culm hydraulic architecture of the bamboo without secondary growth also conforms to the predictions of hydraulic optimality model, with a vessel widening pattern ($b \approx 0.2$) that matches the expected value. However, vessels near the culm base are narrower than expected, which may reflect the constraints on high carbon investment toward the base. As bamboos are monocotyledons without secondary growth and the vessel widening pattern is formed before shoot elongation, there seems to be a predetermined blueprint for their hydraulic construction. At the culm apex, low hydraulic conductivity, water potentials, F_v/F_m and gas exchange parameters suggest severe water stress during the dry season, which may result in carbon imbalance and partly be responsible for top dieback. Moreover, declined maximum positive pressure in the dry season is closely related to culm height reduction after top dieback, which could be caused by insufficient refilling of water storage and xylem embolism. This

study implies the influences of vessel widening pattern and positive pressure decline on the physiological responses of culm top, providing important implications for understanding the bamboo top dieback under increasing drought.

ACKNOWLEDGEMENTS

We acknowledge Yu-Hang Sun and Hong Ma for their assistances in the field. We appreciate the anonymous reviewers and the editors for their valuable suggestions. We also thank the Xishuangbanna Station for Tropical Rain Forest Ecosystem Studies (XSTRFES, Chinese Academy of Sciences) for providing the permission to collect the bamboo samples and logistic support.

CONFLICT OF INTEREST

No conflict of interest is declared.

FUNDING

This research was supported by the National Natural Science Foundation of China (32360258, 32260264, and 31760114), the Yunnan Fundamental Research Projects from Science and Technology Department of Yunnan Province (202201AT070085 and and 202501AT070201), and the Cooperative Research Projects from Chunhui (Spring) Program of Ministry of Education of China (HZKY20220610 and 20200703).

AUTHORS'S CONTRIBUTIONS

SJY and YJZ conceived the ideas and designed the experiment; SJY, WG and JQF

conducted the measurements, collected and analyzed the data; SJY, WG and YJZ wrote the manuscript, and received revision from JLZ, ZXF, PLF and HC.

LITERATURE CITED

Anfodillo T, Carraro V, Carrer M, Fior C, Rossi S. 2006. Convergent tapering of xylem conduits in different woody species. *New Phytologist* **169**: 279-290. doi:10.1111/j.1469-8137.2005.01587.x.

Anfodillo T, Olson ME. 2021. Tree mortality: testing the link between drought, embolism vulnerability, and xylem conduit diameter remains a priority. *Frontiers in Forests and Global Change* **4**: 704670. doi:10.3389/ffgc.2021.704670.

Anfodillo T, Petit G, Crivellaro A. 2013. Axial conduit widening in woody species: a still neglected anatomical pattern. *IAWA Journal* **34**: 352-364. doi:10.1163/22941932-00000030.

Aritsara ANA, Cao KF. 2020. Structural organization in palm stem of *Roystonea regia* and *Archontophoenix alexandrae*. *IAWA Journal* **42**: 64-80. doi:10.1163/22941932-bja10009.

Ault TR. 2020. On the essentials of drought in a changing climate. *Science* **368**: 256-260. doi:10.1126/science.aaz5492.

Banavar JR, Maritan A, Rinaldo A. 1999. Size and form in efficient transportation networks. *Nature* **399**: 130-132. doi:10.1038/20144.

Becker P, Gribben RJ, Lim CM. 2000. Tapered conduits can buffer hydraulic conductance from path-length effects. *Tree Physiology* **20**: 965-967. doi:10.1093/treephys/20.14.965.

Becker P, Gribben RJ, Schulte PJ. 2003. Incorporation of transfer resistance between trancheary elements into hydraulic resistance models for tapered

conduits. *Tree Physiology* **23**: 1009-1019. doi:10.1093/treephys/23.15.1009.

Bettiati D, Petit G, Anfodillo T. 2012. Testing the equi-resistance principle of xylem transport system in a small ash tree: empirical support from anatomical analyses. *Tree Physiology* **32**: 171-177. doi:10.1093/treephys/tpr137.

Brodribb TJ, Bowman DJMS, Nichols S, Delzon S, Burlett R. 2010. Xylem function and growth rate interact to determine recovery rates after exposure to extreme water deficit. *New Phytologist* **188**: 533-542. doi:10.1111/j.1469-8137.2010.03393.x.

Burgess SSO, Pittermann J, Dawson TE. 2006. Hydraulic efficiency and safety of branch xylem increases with height in *Sequoia sempervirens* (D. Don) crowns. *Plant, Cell and Environment* **29**: 229-239. doi: 10.1111/j.1365-3040.2005.01415.x.

Camarero JJ. 2021. Within- versus between-species size effects on drought-induced dieback and mortality. *Tree Physiology* **41**: 679-682. doi:10.1093/treephys/tpaa167.

Cao KF, Yang SJ, Zhang YJ, Brodribb TJ. 2012. The maximum height of grasses is determined by roots. *Ecology Letters* **15**: 666-672. doi:10.1111/j.1461-0248.2012.01783.x.

Choat B, Lahr EC, Melcher PJ, Zwieniecki MA, Holbrook NM. 2005. The spatial pattern of air seeding thresholds in mature sugar maple trees. *Plant, Cell and Environment* **28**: 1082-1089. doi:10.1111/j.1365-3040.2005.01336.x.

Choat B, Sack L, Holbrook NM. 2007. Diversity of hydraulic traits in nine *Cordia* species growing in tropical forests with contrasting precipitation. *New Phytologist* **175**: 686-698. doi:10.1111/j.1469-8137.2007.02137.x.

Cochard H, Ewers FW, Tyree MT. 1994. Water relations of a tropical vine like bamboo (*Rhipidocladum racemiflorum*): root pressures, vulnerability to cavitation and seasonal changes in embolisms. *Journal of Experimental Botany* **45**: 1085-1089. doi:10.1093/jxb/45.8.1085.

Comstock JP, Sperry JS. 2000. Theoretical considerations of optimal conduit length for water transport in vascular plants. *New Phytologist* **148**: 195-218. doi:10.1046/j.1469-8137.2000.00763.x.

Dai AG. 2013. Increasing drought under global warming in observations and models. *Nature Climate Change* **3**: 52-58. doi:10.1038/nclimate1633.

Davis SD, Ewers FW, Sperry JS, Portwood KA, Crocker MC, Adams GC. 2002. Shoot dieback during prolonged drought in *Ceanothus* (Rhamnaceae) chaparral of California: a possible case of hydraulic failure. *American Journal of Botany* **89**: 820-828. doi:10.3732/ajb.89.5.820.

Domec J-C, Lachenbruch B, Meinzer FC, Woodruff DR, Warren JM, McCulloh KA. 2008. Maximum height in a conifer is associated with conflicting requirements for xylem design. *Proceedings of the National Academy of Sciences, USA* **105**: 12069-12074. doi:10.1073/pnas.0710418105.

Dória LC, Podadera DS, Lima RS, Lens F, Marcati CR. 2019. Axial sampling height outperforms site as predictor of wood trait variation. *IAWA Journal* **40**: 191-214. doi:10.1163/22941932-40190245.

Drobnitch ST, Comas LH, Flynn N, Caballero JI, Barton RW, Wenz J, Person T, Bushey J, Jahn CE, Gleason SM. 2021. Drought-induced root pressure in *Sorghum bicolor*. *Frontiers in Plant Science* **12**: 571072. doi:10.3389/fpls.2021.571072.

Echeverría A, Anfodillo T, Soriano D, Rosell JA, Olson ME. 2019. Constant theoretical conductance via changes in vessel diameter and number with height growth in *Moringa oleifera*. *Journal of Experimental Botany* **70**: 5765-5772. doi:10.1093/jxb/erz329.

Ellsworth DS, Reich PB. 1993. Canopy structure and vertical patterns of photosynthesis and related leaf traits in a deciduous forest. *Oecologia* **96**: 169-178. doi:10.1007/BF00317729.

Fajardo A, Martínez-Pérez C, Cervantes-Alcayde MA, Olson ME. 2020. Stem length, not climate, controls vessel diameter in two tree species across a sharp precipitation gradient. *New Phytologist* **225**: 2347-2355. doi:10.1111/nph.16287.

Fan ZX, Cao KF, Becker P. 2009. Axial and radial variations in xylem anatomy of angiosperm and conifer trees in Yunnan, China. *IAWA Journal* **30**: 1-13. doi:10.1163/22941932-90000198.

Fang LD, Ning QR, Guo JJ, Gong XW, Zhu JJ, Hao GY. 2021. Hydraulic limitation underlies the dieback of *Populus pseudo-simonii* trees in water-limited areas of northern China. *Forest Ecology and Management* **483**: 118764. doi:10.1016/j.foreco.2020.118764.

Fichot R, Barigah TS, Chamaillard S, Thiec DL, Laurans F, Cochard H, Brignolas F. 2010. Common trade-offs between xylem resistance to cavitation and other physiological traits do not hold among unrelated *Populus deltoides* × *Populus nigra* hybrids. *Plant, Cell & Environment* **33**: 1553-1568. doi:10.1111/j.1365-3040.2010.02164.x.

Fu PL, Zhang Y, Zhang YJ, Finnegan PM, Yang SJ, Fan ZX. 2022. Leaf gas exchange and water relations of the woody desiccation-tolerant *Paraboea*

rufescens during dehydration and rehydration. *AoB PLANTS* **14**: plac033. doi:10.1093/aobpla/plac033.

Gleason SM, Wiggans DR, Bliss CA, Young JS, Cooper M, Willi KR, Comas LH. 2017. Embolized stems recover overnight in *Zea mays*: The role of soil water, root pressure, and nighttime transpiration. *Frontiers in Plant Science* **8**: 662. doi:10.3389/fpls.2017.00662.

Hentschel R, Rosner S, Kayler ZE, Andreassen K, Borjia I, Solberg S, Tveito OE, Priesack E, Gessler A. 2014. Norway spruce physiological and anatomical predisposition to dieback. *Forest Ecology and Management* **322**: 27-36. doi:10.1016/j.foreco.2014.03.007.

Hochberg U, Herrera JC, Cochard H, Badel E. 2016. Short-time xylem relaxation results in reliable quantification of embolism in grapevine petioles and sheds new light on their hydraulic strategy. *Tree Physiology* **36**: 748-755. doi:10.1093/treephys/tpv145.

Hölttä T, Mencuccini M, Nikinmaa E. 2011. A carbon cost–gain model explains the observed patterns of xylem safety and efficiency. *Plant, Cell & Environment* **34**: 1819-1834. doi:10.1111/j.1365-3040.2011.02377.x.

Jacobsen AL, Brandon Pratt R, Tobin MF, Hacke UG, Ewers FW. 2012. A global analysis of xylem vessel length in woody plants. *American Journal of Botany* **99**:1583-1591. doi:10.3732/ajb.1200140.

James S, Meinzer F, Goldstein G, Woodruff D, Jones T, Restom T, Mejia M, Clearwater M, Camanello P. 2003. Axial and radial water transport and internal water storage in tropical forest canopy trees. *Oecologia* **134**: 37-45. doi:10.1007/s00442-002-1080-8.

Jin N, Yu XC, Dong JL, Duan MC, Mo YX, Feng LY, Bai R, Zhao JL, Song J, Dossa GGO, Lu HZ. 2024. Vertical variation in leaf functional traits of *Parashorea chinensis* with different canopy layers. *Frontiers in Plant Science* **15**: 1335524. doi:10.3389/fpls.2024.1335524.

Kenzo T, Inoue Y, Yoshimura M, Yamashita M, Tanaka-Oda A, Ichie T. 2015. Height-related changes in leaf photosynthetic traits in diverse Bornean tropical rain forest trees. *Oecologia* **177**: 191-202. doi:10.1007/s00442-014-3126-0.

Kenzo T, Yoneda R, Sano M, Araki M, Shimizu A, Tanaka-oda A, Chann S. 2012. Variations in leaf photosynthetic and morphological traits with tree height in various tree species in Cambodian tropical dry evergreen forest. *Japan Agricultural Research Quarterly* **46**: 167-180. doi:10.6090/jarq.46.167.

Kiorapostolou N, Camarero JJ, Carrer M, Sterck F, Brigita B, Sanguesa-Barreda G, Petit G. 2020. Scots pine trees react to drought by increasing xylem and phloem conductivities. *Tree Physiology* **40**: 774-781. doi:10.1093/treephys/tpaa033.

Kiorapostolou N, Galiano-Pérez L, von Arx G, Gessler A, Petit G. 2018. Structural and anatomical responses of *Pinus sylvestris* and *Tilia platyphyllos* seedlings exposed to water shortage. *Trees* **32**: 1211-1218. doi:10.1007/s00468-018-1703-2.

Knipfer T, Cuneo IF, Brodersen CR, McElrone AJ. 2016. In Situ visualization of the dynamics in xylem embolism formation and removal in the absence of root pressure: a study on excised grapevine stems. *Plant Physiology* **171**: 1024-1036. doi:10.1104/pp.16.00136.

Knipfer T, Eustis A, Brodersen CR, Walker MA, McElrone A. 2015. Grapevine

species from varied native habitats exhibit differences in embolism formation/repair associated with leaf gas exchange and root pressure. *Plant, Cell & Environment* **38**: 1503-1513. doi:10.1111/pce.12497.

Koch GW, Sillett SC, Jennings GM, Davis SD. 2004. The limits to tree height. *Nature* **428**: 851-854. doi:10.1038/nature02417.

Koçillari L, Olson ME, Suweis S, Rocha RP, Lovison A, Cardin F, Dawson TE, Echeverría A, Fajardo A, Lechthaler S, Martinez-Perez C, Marcati CR, Chung KF, Rosell JA, Segovia-Rivas A, Williams CB, Petrone-Mendoza E, Rinaldo A, Anfodillo T, Banavar JR, Maritan A. 2021. The widened pipe model of plant hydraulic evolution. *Proceedings of the National Academy of Sciences, USA* **118**: e2100314118. doi:10.1073/pnas.2100314118.

Kongjarat W, Han L, Aritsara ANA, Zhang SB, Zhao GJ, Zhang YJ, Maenpuen P, Li YM, Zou YK, Li MY, Li XN, Tao LB, Chen YJ. 2024. Hydraulic properties and drought response of a tropical bamboo (*Cephalostachyum pergracile*). *Plant Diversity* **46**: 406-415. doi:10.1016/j.pld.2023.12.003.

Lechthaler S, Kiorapostolou N, Pitacco A, Anfodillo T, Petit G. 2020. The total path length hydraulic resistance according to known anatomical patterns: what is the shape of the root-to leaf tension gradient along the plant longitudinal axis? *Journal of Theoretical Biology* **502**: 110369. doi:10.1016/j.jtbi.2020.110369.

Lechthaler S, Turnbull TL, Gelmini Y, Pirotti F, Anfodillo T, Adams MA, Petit G. 2019. A standardization method to disentangle environmental information from axial trends of xylem anatomical traits. *Tree Physiology* **39**: 495-502. doi:10.1093/treephys/tpy110.

Lintunen A, Kalliokoski T. 2010. The effect of tree architecture on conduit diameter

and frequency from small distal roots to branch tips in *Betula pendula*, *Picea abies* and *Pinus sylvestris*. *Tree Physiology* **30**: 1433-1447. doi:10.1093/treephys/tpq085.

Mencuccini M, Hölttä T, Petit G, Magnani F. 2007. Sanio's laws revisited. Size-dependent changes in the xylem architecture of trees. *Ecology Letters* **10**: 1084-1093. doi:10.1111/j.1461-0248.2007.01104.x.

Michaud JM, Mocko K, Schenk HJ. 2024. Positive pressure in bamboo is generated in stems and rhizomes, not in roots. *AoB Plants* **16**: plae040. doi:10.1093/aobpla/plae040.

Mueller-Dombois D. 1988. Forest decline and dieback-A global ecological problem. *Trends in Ecology & Evolution* **3**: 310-312. doi:10.1016/0169-5347(88)90108-5.

Nardini A, Battistuzzo M, Savi T. 2013. Shoot desiccation and hydraulic failure in temperate woody angiosperms during an extreme summer drought. *New Phytologist* **200**: 322-329. doi:10.1111/nph.12288.

Nolan RH, Gauthey A, Losso A, Medlyn BE, Smith R, Chhajed SS, Fuller K, Song M, Li X, Beaumont LJ, Boer MM, Wright IJ, Choat B. 2021. Hydraulic failure and tree size linked with canopy die-back in eucalypt forest during extreme drought. *New Phytologist* **230**: 1354-1365. doi:10.1111/nph.17298.

Olson ME, Anfodillo T, Gleason SM, McCulloh KA. 2021. Tip-to-base xylem conduit widening as an adaptation: cause, consequences, and empirical priorities. *New Phytologist* **229**: 1877-1893. doi:10.1111/nph.16961.

Olson ME, Anfodillo T, Rosell JA, Petit G, Crivellaro A, Isnard S, León-Gómez C, Alvarado-Cárdenas LO, Castorena M. 2014. Universal hydraulics of the flowering plants: vessels diameter scales with stem length across angiosperm

lineages, habits and climates. *Ecology Letters* **17**: 988-997. doi:10.1111/ele.12302.

Olson ME, Rosell JA. 2013. Vessel diameter-stem diameter scaling across woody angiosperms, and the ecological causes of xylem vessel diameter variation. *New Phytologist* **197**: 1204-1213. doi:10.1111/nph.12097.

Olson ME, Rosell JA, Leon C, Zamora S, Weeks A, Alvarado-Cardenas LO, Cacho NI, Grant J. 2013. Convergent vessel diameter-stem diameter scaling across five clades of new and old world eudicots from desert to rain forest. *International Journal of Plant Sciences* **174**: 1062-1078. doi:10.1086/671432.

Olson ME, Soriano D, Rosell JA, Anfodillo T, Donoghue MJ, Edwards EJ, Leon-Gomez C, Dawson T, Martinez JJC, Castorena M, Echeverría A, Espinosa CI, Fajardo A, Gazol A, Isnard S, Lima RS, Marcati CR, Mendez-Alonzo R. 2018. Plant height and hydraulic vulnerability to drought and cold. *Proceedings of the National Academy of Sciences, USA* **115**: 7551-7556. doi:10.1073/pnas.1721728115.

Pellizzari E, Camarero JJ, Gazol A, Sanguesa-Barreda G, Carrer M. 2016. Wood anatomy and carbon-isotope discrimination support long-term hydraulic deterioration as a major cause of drought-induced dieback. *Global Change Biology* **22**: 2125-2137. doi:10.1111/gcb.13227.

Petit G, Anfodillo T. 2009. Plant physiology in theory and practice: an analysis of the WBE model for vascular plants. *Journal of Theoretical Biology* **259**: 1-4. doi:10.1016/j.jtbi.2009.03.007.

Petit G, Anfodillo T, De Zan C. 2009. Degree of tapering of xylem conduits in stems and roots of small *Pinus cembra* and *Larix decidua* trees. *Botany* **87**: 501-508.

doi:10.1139/B09-025.

Petit G, Anfodillo T, Mencuccini M. 2008. Tapering of xylem conduits and hydraulic limitations in sycamore (*Acer pseudoplatanus*) trees. *New Phytologist* **177**: 653-664. doi:10.1111/j.1469-8137.2007.02291.x.

Petit G, Crivellaro A. 2014. Comparative axial widening of phloem and xylem conduits in small woody plants. *Trees* **28**: 915-921. doi:10.1007/s00468-014-1006-1.

Petit G, DeClerck FAJ, Carrer M, Anfodillo T. 2014. Axial vessel widening in arborescent monocots. *Tree Physiology* **34**: 137-145. doi:10.1093/treephys/tpt118.

Petit G, Pfautsch S, Anfodillo T, Adams MA. 2010. The challenge of tree height in *Eucalyptus regnans*: when xylem tapering overcomes hydraulic resistance. *New Phytologist* **187**: 1146-1153. doi:10.1111/j.1469-8137.2010.03304.x.

Pfautsch S. 2016. Hydraulic anatomy and function of trees- basics and critical developments. *Current Forestry Reports* **2**: 236-248. doi:10.1007/s40725-016-0046-8.

Pfautsch S, Aspinwall MJ, Drake JE, Chacon-Dória L, Langelaan RJA, Tissue DT, Tjoelker MG, Lens F. 2018. Traits and trade-offs in whole-tree hydraulic architecture along the vertical axis of *Eucalyptus grandis*. *Annals of Botany* **121**: 129-141. doi:10.1093/aob/mcx137.

Pivovaroff AL, Sack L, Santiago LS. 2014. Coordination of stem and leaf hydraulic conductance in southern California shrubs: a test of the hydraulic segmentation hypothesis. *New Phytologist* **203**: 842-850. doi: 10.1111/nph.12850.

Plavcová L, Hoch G, Morris H, Ghiasi S, Jansen S. 2016. The amount of parenchyma and living fibers affects storage of nonstructural carbohydrates in young stems and

roots of temperate trees. *American Journal of Botany* **103**: 603-612. doi:10.3732/ajb.1500489.

Prendin AL, Mayr S, Beikircher B, von Arx G, Petit G. 2018a. Xylem anatomical adjustments prioritize hydraulic efficiency over safety as Norway spruce trees grow taller. *Tree Physiology* **38**: 1088-1097. doi:10.1093/treephys/tpy065.

Prendin AL, Petit G, Fonti P, Rixen C, Dawes MA, von Arx G. 2018b. Axial xylem architecture of *Larix decidua* exposed to CO_2 enrichment and soil warming at the tree line. *Functional Ecology* **32**: 273-287. doi:10.1111/1365-2435.12986.

Rita A, Pericolo O, Tumajer J, Ripullone F, Gentilesca T, Saracino A, Borghetti M. 2024. Tip-to-base conduit widening remains consistent across cambial age and climates in *Fagus sylvatica* L. *Tree Physiology* **44**: tpae080. doi:10.1093/treephys/tpae080.

Rood SB, Patiño S, Coombs K, Tyree MT. 2000. Branch sacrifice: cavitation-associated drought adaptation of riparian cottonwoods. *Trees* **14**: 248-257. doi:10.1007/s004680050010.

Rosell JA, Olson ME, Anfodillo T. 2017. Scaling of xylem vessel diameter with plant size: cause, predictions and outstanding questions. *Current Forestry Reports* **3**: 46-59. doi:10.1007/s40725-017-0049-0.

Rosner S, Svetlik J, Andreassen K, Borja I, Dalsgaard L, Evans R, Luss S, Tveito OE, Solberg S. 2016. Novel hydraulic vulnerability proxies for a boreal conifer species reveal that opportunists may have lower survival prospects under extreme climatic events. *Frontiers in Plant Science* **7**: 831. doi:10.3389/fpls.2016.00831.

Saha S, Holbrook NM, Montti L, Goldstein G, Cardinot GK. 2009. Water relations of *Chusquea ramossissima* and *Merostachys claussenii* in Iguazu National Park, Argentina. *Plant Physiology* **149**: 1992-1999. doi:10.1104/pp.108.129015.

Savi T, Casolo V, Dal Borgo A, Rosner S, Torboli V, Stenni B, Bertoncin P, Martello S, Pallavicini A, Nardini A. 2019. Drought-induced dieback of *Pinus nigra*: a tale of hydraulic failure and carbon starvation. *Conservation Physiology* **7**: coz012. doi:10.1093/conphys/coz012.

Schenk HJ, Jansen S, Hölttä T. 2021. Positive pressure in xylem and its role in hydraulic function. *New Phytologist* **230**: 27-45. doi:10.1111/nph.17085.

Singh S. 2016. Root pressure: getting to the root of pressure. *Progress in Botany* **77**: 105-150. doi:10.1007/978-3-319-25688-7_3.

Soriano D, Echeverría A, Anfodillo T, Rosell JA, Olson ME. 2020. Hydraulic traits vary as the results of tip-to-base conduit widening in vascular plants. *Journal of Experimental Botany* **71**: 4232-4242. doi:10.1093/jxb/eraa157.

Stiller V, Lafitte HR, Sperry JS. 2003. Hydraulic properties of rice and the response of gas exchange to water stress. *Plant Physiology* **132**: 1698-1706. doi:10.1104/pp.102.019851.

Subczynski WK, Hopwood LE, Hyde JS. 1992. Is the mammalian cell plasma membrane a barrier to oxygen transport? *Journal of General Physiology* **100**: 69-87. doi:10.1085/jgp.100.1.69.

Trugman AT, Detti M, Bartlett MK, Medvigy D, Anderegg WRL, Schwalm C, Schaffer B, Pacala S. 2018. Tree carbon allocation explains forest drought-kill and recovery patterns. *Ecology Letters* **21**: 1552-1560. doi:10.1111/ele.13136.

Tyree MT, Zimmermann MH. 2002. *Xylem structure and the ascent of sap*. Berlin, Heidelberg: Springer Verlag. doi:10.1007/978-3-662-04931-0.

Xu GQ, Chen TQ, Liu SS, Ma J, Li Y. 2023. Within-crown plasticity of hydraulic properties influence branch dieback patterns of two woody plants under experimental drought conditions. *The Science of the Total Environment* **854**:158802. doi:10.1016/j.scitotenv.2022.158802.

West GB, Brown JH, Enquist BJ. 1999. A general model for the structure and allometry of plant vascular systems. *Nature* **400**: 664-667. doi:10.1038/23251.

Williams CB, Anfodillo T, Crivellaro A, Lazzarin M, Dawson TE, Koch GW. 2019. Axial variation of xylem conduits in the Earth's tallest trees. *Trees* **33**: 1299-1311. doi:10.1007/s00468-019-01859-w.

Williams CB, Næsborg RR, Ambrose AR, Baxter WL, Koch GW, Dawson TE. 2021. The dynamics of stem water storage in the tops of Earth's largest trees-*Sequoiadendron giganteum*. *Tree Physiology* **41**: 2262-2278. doi:10.1093/treephys/tpab078.

Williams CB, Naesborg RR, Dawson TE. 2017. Coping with gravity: the foliar water relations of giant sequoia. *Tree Physiology* **37**: 1312-1326. doi:10.1093/treephys/tpx074.

Woodruff DR, Bond BJ, Meinzer FC. 2004. Does turgor limit growth in tall trees? *Plant, Cell & Environment* **27**: 229-236. doi:10.1111/j.1365-3040.2003.01141.x.

Yang DM, Zhang YS, Zhou D, Zhang YJ, Peng GQ, Tyree MT. 2021. The hydraulic architecture of an arborescent monocot: ontogeny-related adjustments in vessel size and leaf area compensate for increased resistance. *New Phytologist* **231**: 273-284. doi:10.1111/nph.17294.

Yang DM, Zhou W, Wang XL, Zhao M, Zhang YJ, Tyree MT, Peng GQ. 2024. An analytical complete model of root pressure generation: Theoretical bases for studying hydraulics of bamboo. *Plant, Cell and Environment* **47**: 59-71. doi:10.1111/pce.14730.

Yang SJ, Zhang YJ, Goldstein G, Sun M, Ma RY, Cao KF. 2015. Determinants of water circulation in a woody bamboo species: afternoon use and night-time recharge of culm water storage. *Tree Physiology* **35**: 964-974. doi:10.1093/treephys/tpv071.

Yang SJ, Zhang YJ, Sun M, Goldstein G, Cao KF. 2012. Recovery of diurnal depression of leaf hydraulic conductance in a subtropical woody bamboo species: embolism refilling by nocturnal root pressure. *Tree Physiology* **32**: 414-422. doi:10.1093/treephys/tps028.

Zhang YJ, Meinzer FC, Hao GY, Scholz FG, Bucci SJ, Takahashi FSC, Villalobos-Vega R, Giraldo JP, Cao KF, Hoffmann, WA, Goldstein G. 2009. Size-dependent mortality in a Neotropical savanna tree: the role of height-related adjustments in hydraulic architecture and carbon allocation. *Plant, Cell & Environment* **32**: 1456-1466. doi:10.1111/j.1365-3040.2009.02012.x.

Figure Legends

Figure 1. Variation of hydraulically-weighted mean vessel diameter (D_h) with the distance from the culm tip (L) (**a**). Linear relationship between Log_{10} (D_h) and Log_{10} (L) is shown in the inset. Hollow symbols were removed from the Log-Log correlation. Solid, dashed and dotted lines are the regression line, the 95% CIs (confidence intervals) and 95% PIs (prediction intervals), respectively (details in Table 1). Anatomical images (**b, c, d,** and **e**) of bamboo culm cross-sections are illustrated using light microscopy along a vertical gradient within a single culm of a tall *D. membranaceus* (D1). The distance from the culm tip (L) that theses collected samples is shown at the bottom of each image, respectively. Scale bars=200 μm.

Figure 2. Variation of vessel traits in cross-section of culm wall with different relative distance from the culm tip. The vessel traits include (**a**) vessel area ratio, (**b**) vessel density, (**c**) vessel number, and (**d**) maximum vessel diameter (D_{max}). The area percentage relationship between vessel and parenchyma of the total area of each cross-section is shown in the inset (**a**). Solid, dashed and dotted lines are the regression line, the 95% CIs and 95% PIs, respectively.

Figure 3. Variation of hydraulic traits in cross-section of culm wall with different relative distance from the culm tip. The hydraulic traits include (**a**) theoretical hydraulic conductivity (K_h), (**b**) theoretical sapwood-specific hydraulic conductivity (K_s), (**c**) theoretical cumulated total hydraulic resistance (R_{tot}) from the basal culm upwards, and (**d**) wood density (WD). The hydraulic resistance of each internode (R) is shown in the inset (**c**). Solid, dashed and dotted lines are the regression line, the 95% CIs and 95%

PIs, respectively.

Figure 4. Variations in leaf chlorophyll fluorescence, morphology and water potential with different relative distance from the culm tip during the dry season. (**a**) maximum quantum yield of photosystem II (F_v/F_m), (**b**) leaf dry mass per unit area (LMA), single leaf size (leaf area, A_L) (the inset), (c) leaf predawn water potential (Ψ_{pre}), and (**d**) leaf midday water potential (Ψ_{mid}). Error bars represent variation (mean ± SE) among different measurements within the height interval. Solid, dashed and dotted lines are the regression line, the 95% CIs and 95% PIs, respectively.

Figure 5. Variations in leaf photosynthetic gas exchange with different relative distance from the culm tip during the dry season. (**a**) maximum photosynthetic rate (A_{max}), (**b**) stomatal conductance (g_s), (**c**) transpiration rate (E), and (**d**) instantaneous water-use efficiency (WUE_i). Error bars represent variation (mean ± SE) among different measurements within the height interval. Solid, dashed and dotted lines are the regression line, the 95% CIs and 95% PIs, respectively.

Figure 6. Correlation between measured culm height and maximum positive pressure. The measured height of culm apex after top dieback in the dry season (Measured-H_{dry}, black circle), measured height of culm apex before top dieback in the wet season (Measured-H_{wet}, white circle), and heights calculated by maximum positive pressure in the dry (Calculated-H_{dry}, black triangle) and wet (Calculated-H_{wet}, white triangle) seasons are shown, respectively. The maximum positive pressure measured during the dry (black bar) and wet (white bar) seasons is shown in the inset. T-tests (**, $P < 0.01$;

ns, $P > 0.05$) were used to determine the statistical difference. All data are presented as mean ± SE.

Table 1. Parameters of the linear relationship $\mathrm{Log}_{10}(D_h) = a + b\mathrm{Log}_{10}(L)$ along the culm of the sampled bamboo (*D. membranaceus*) with three different individuals (D1, D2, and D3). D_h is hydraulically weighted mean vessel diameter, L is distance from the culm tip. N is the number of sampling points for the Log-Log correlation along the bamboo culm. The 95% CIs of a and b are in parentheses, respectively.

ID	N	a	b	R^2	P
D1	24	1.85 (1.82-1.87)	0.17 (0.16-0.18)	0.95	< 0.0001
D2	27	1.87 (1.85-1.89)	0.16 (0.15-0.16)	0.94	< 0.0001
D3	29	1.83 (1.81-1.85)	0.17 (0.17-0.18)	0.96	< 0.0001
D1 + D2 + D3	80	1.84 (1.83-1.85)	0.17 (0.17-0.18)	0.95	< 0.0001

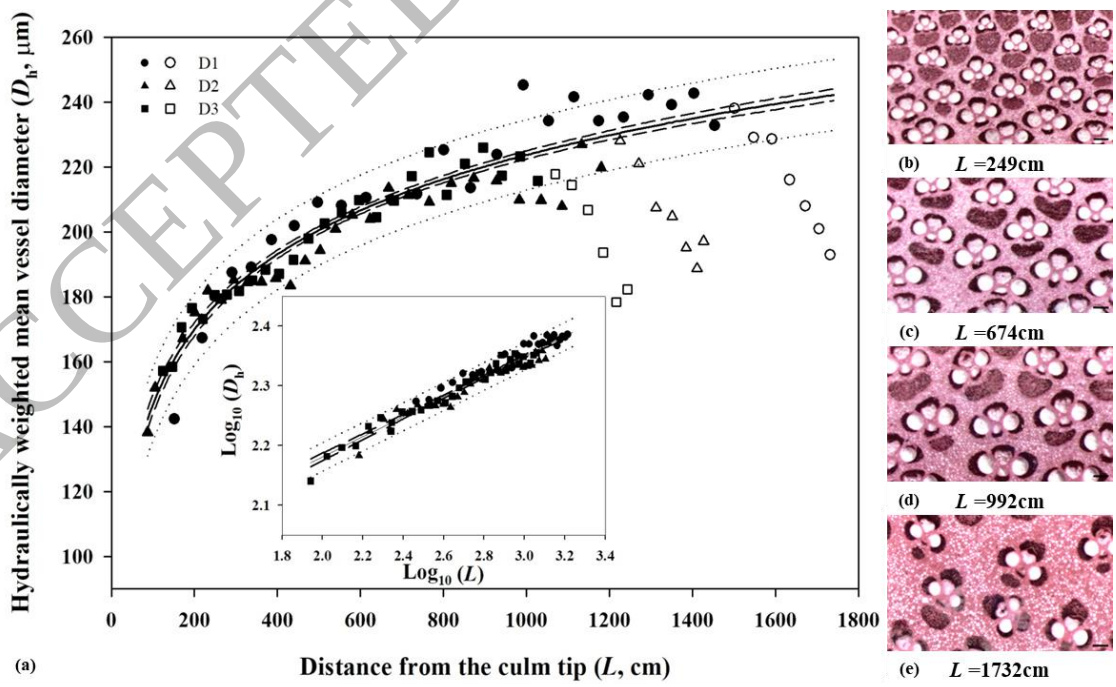

Figure 1
148x91 mm (x DPI)

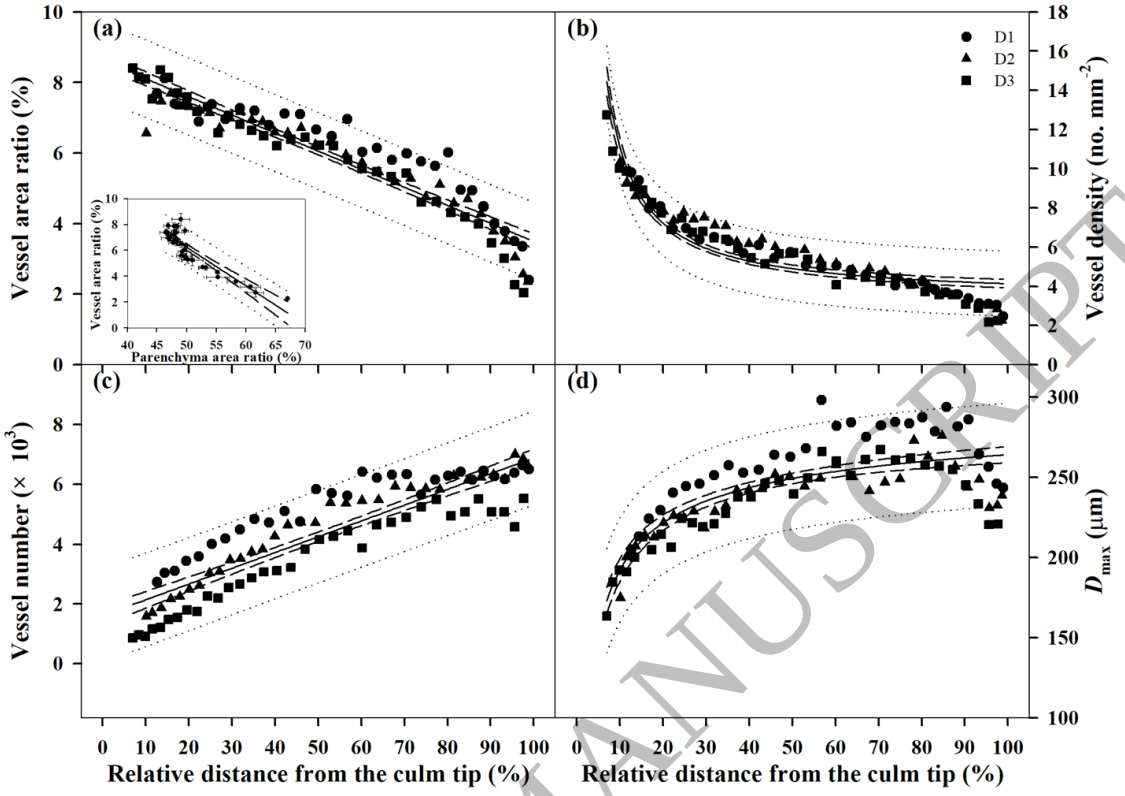

Figure 2
148x105 mm (x DPI)

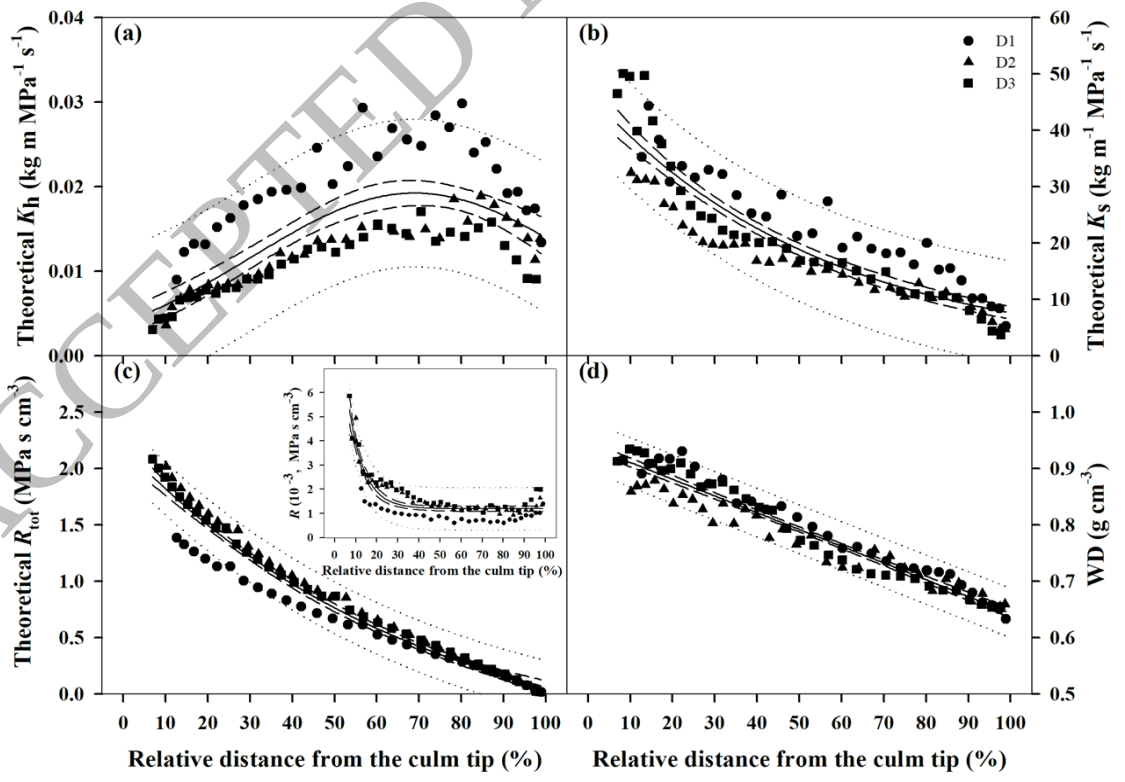

Figure 3
148x105 mm (x DPI)

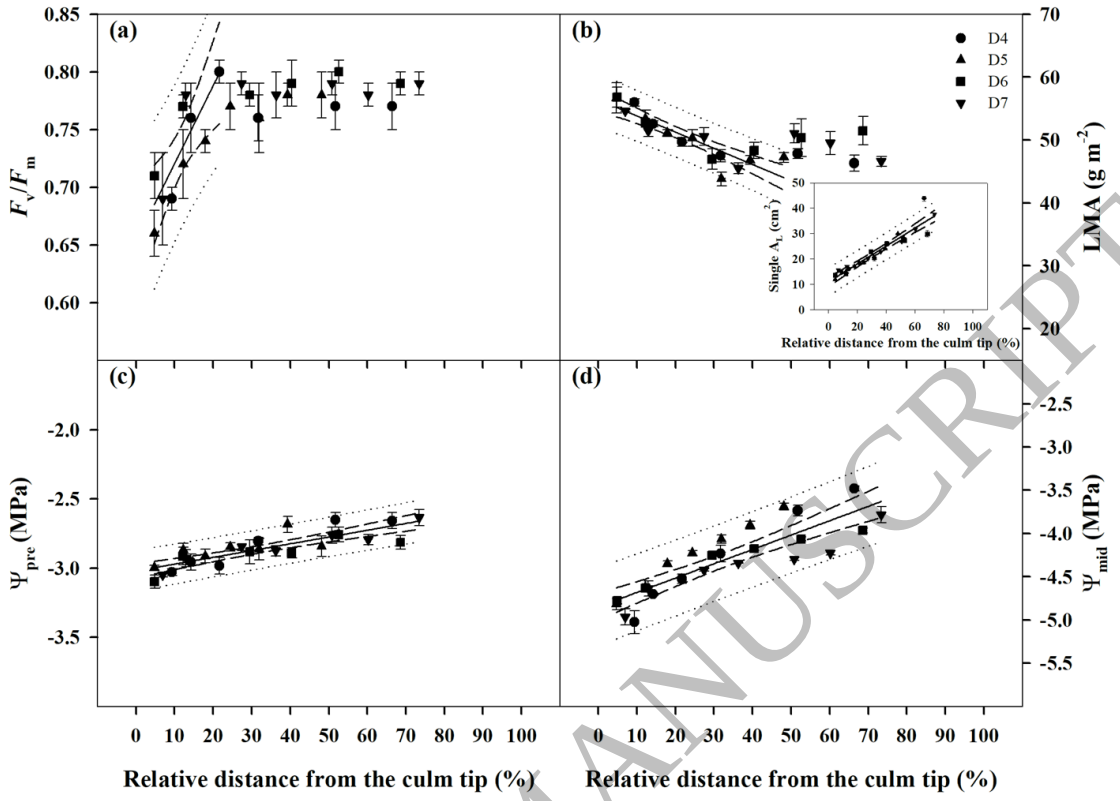

Figure 4
148x105 mm (x DPI)

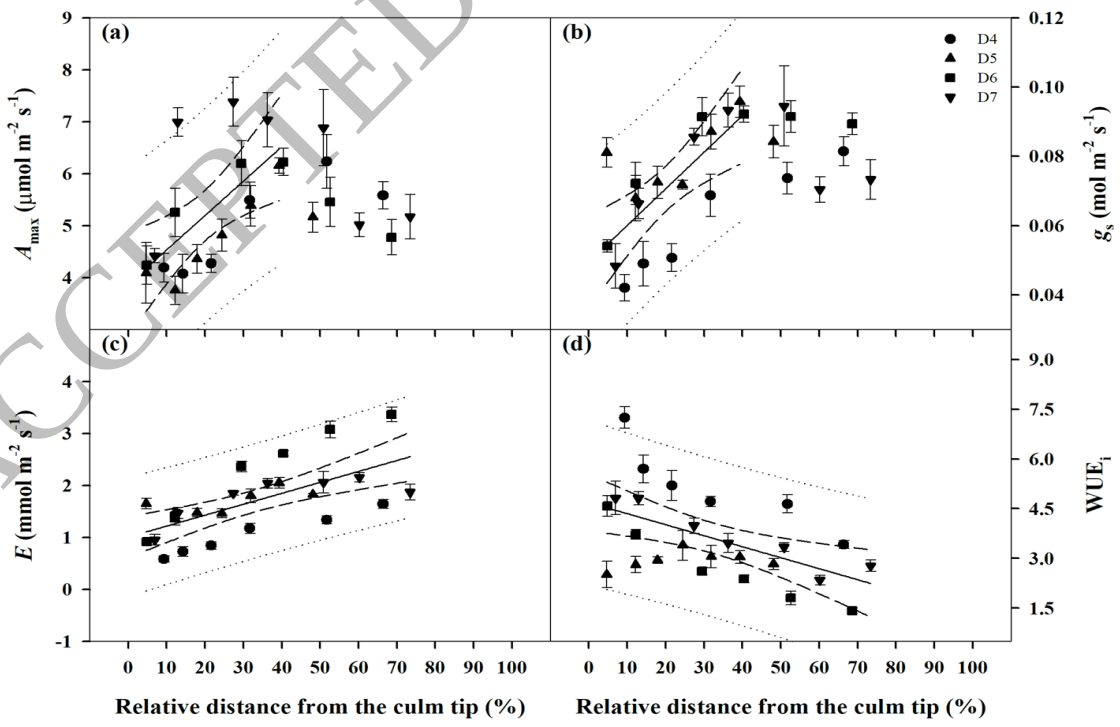

Figure 5
148x104 mm (x DPI)

1

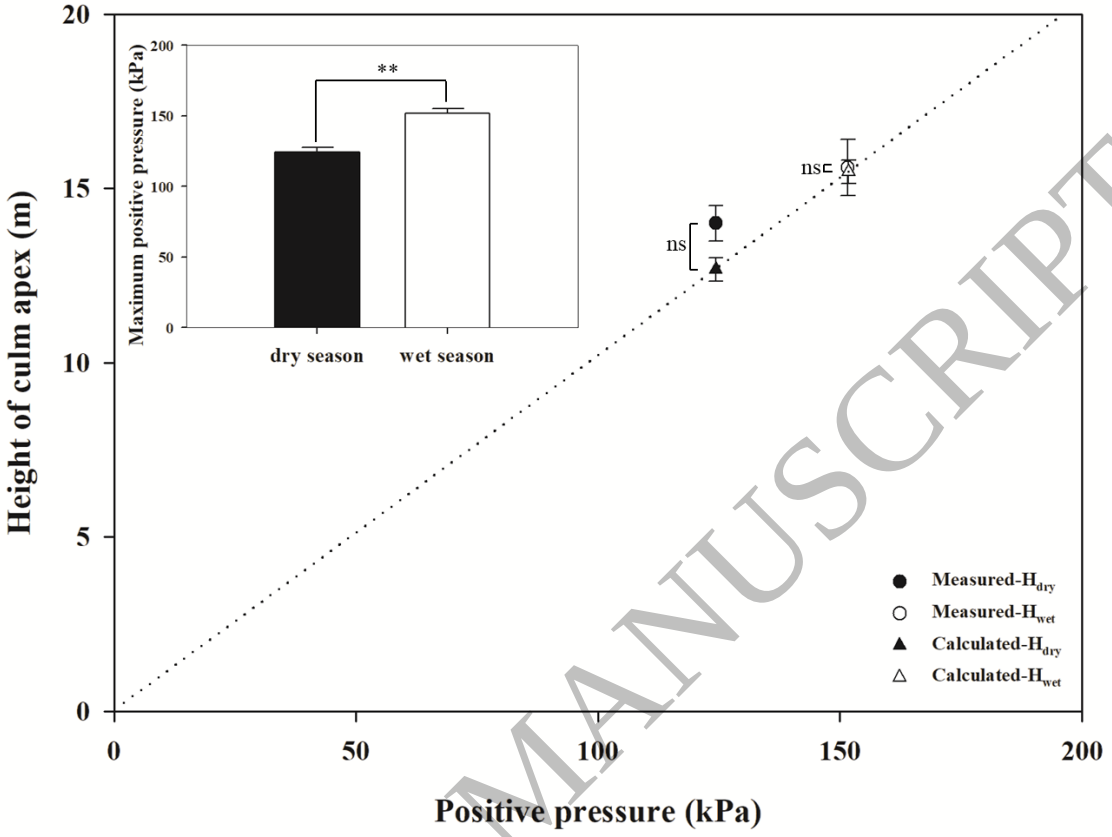

2

3 *Figure 6*
4 *148x111 mm (x DPI)*